University of Zurich
Department of Physics

Characterization of NaI(Tl) detectors for a radioactive decay rate modulation search experiment

Bachelor Thesis in Physics

Magnus Gienal

Supervised by

Prof. Dr. Laura Baudis
Dr. Alexander Kish
Peter Barrow

February 8, 2017

Abstract

An experiment dedicated to the observation of modulations in radioactive decay rates is being set up at the University of Zurich. The experiment uses eight NaI(Tl) scintillators to detect photons originating from a radioactive decay. This thesis covers two key points connected to these detectors. The first part focuses on built-in light-emitting diodes, which serve for the calibration of the photomultiplier tubes and as an indicator for changes in amplification during the long-term run of the modulation experiment. The functionality of this sub-system was tested, and it was found that the identification of test pulses works as intended. In the second part, the sensitivity of the detectors to variations in the atmospheric pressure was explored, observing a β-decaying ^{137}Cs source. A setup different from the original one had to be used. Covering a large range of pressure settings (0.5 to 1.5 bar), the results show a dependency of the measured decay rates on the pressure level. This effect could not be fully explained, apart from the observation that it originates from source-related photons. A second measurement at values closer to operational conditions does not show this effect. However, the fluctuations of the decay rates are at or above the desired limit. Therefore, variations in pressure and their effect on measured decay rates need to be accounted for in future experiments.

Contents

List of Abbreviations

C.L.	Confidence level
^{137}Cs	Radioactive isotope of the element caesium with mass number 137
DM	Dark Matter
LED	Light-emitting diode
LNGS	Gran Sasso National Underground Laboratory, Italy
ModuDAQ	Special LabView project built for the modulation experiment for data acquisition
NaI(Tl)	Thalium-doped sodium iodide, material used in scintillation detectors
PMT	Photomultiplier tube
ROOT	Programming language developed at CERN used in particle physics
UZH	University of Zurich

Acknowledgments

I would like to thank my daily supervisor Peter Barrow, who introduced me to the project and helped me with the work in the lab. He was always available to answer questions and lent a helping hand whenever I stumbled across a problem. I would also like to thank Dr. Alex Kish, who helped me working on the analysis of the collected data and reviewed my thesis. Furthermore, I would like to thank Prof. Dr. Laura Baudis for the opportunity to work in her research group for my bachelor thesis.

Another thanks goes out to all the people from the collaboration of the modulation experiment. The atmosphere was very friendly and helpful and made it uncomplicated to join the experiment. At last, I want to thank the staff of the electronics workshop of the Department of Physics, which helped me on technical problems while working with the LEDs.

Chapter 1

Introduction

Since the discovery of radioactivity in 1896, scientists have always studied the behaviour of radioactive elements. The nowadays widely accepted formulation of the radioactive decay law is described in chapter 2. The statistical process of a decaying source is linked to the decay constant, which is stated to be a property of the radioactive element. However, some scientists recently raised the question on the nature of the decay constant and presented evidence for a time-dependent parameter and observation of decay rate modulations. An overview of some publications on this topic is given in chapter 2.

In order to investigate these modulation effects, an experiment was designed to observe the activity of multiple radioactive sources continuously for at least one year, because the found modulations have a period of one year. Four identical setups will be installed at different geographical locations (in Switzerland, the Netherlands, the USA and Brazil). Apart from decay rates, the experiment will also precisely monitor various external parameters, e.g. temperature, atmospheric pressure and humidity. The modulation experiment is introduced in chapter 3 along with a description of its main components.

As a part of the installation and preliminary tests of the modulation experiment, this thesis focused on the following points:

1. Exploring the functionality of the LED test pulse tagging
2. Investigating the sensitivity of the detectors to pressure fluctuations

In the first task, the implemented indicator system for dead-time measurements and detector calibration was examined using a built-in feature of the NaI(Tl) detectors. A light-emitting diode (LED) sends test light pulses onto the photomultiplier tube (PMT), which get detected like real events. By comparison over time, they serve as an indicator for changes in PMT gain and can be used for calibration. The experimental setup is designed to distinguish LED from normal events by bit-manipulating of processed data. The functionality of this LED-tagging was tested in the scope of this thesis. The procedure and results are presented in chapter 4.

The second task laid focus on one of the external effects that could influence the decay rate measurement. An experiment was set up to measure the decay rates of the radioactive source ^{137}Cs while varying the ambient pressure around it to explore the dependency of the results on the level of pressure. Chapter 5 presents the setup and the results of these measurements.

The obtained results of both tasks are discussed in chapter 6, along with the derived conclusions and the constraints of the results to future measurements within the modulation experiment.

Chapter 2

Modulation in radioactive decays

This chapter gives an overview on the underlying principles of radioactive decays and presents previous experiments, which claimed to measure modulations in the decay rate of various radioactive sources, but also publications rejecting these claims. The possible connection of decay rate modulations to the search for dark matter particles is also explained.

2.1 Radioactive decays

Radioactivity was first discovered by Henri Becquerel in 1896, while he was studying Wilhelm Röntgen's X-ray radiation. Becquerel found out that there are elements which naturally emit a new form of radiation, different to the one observed by Röntgen [10]. Today, radioactive decay describes the process of an atom's nucleus losing energy by emitting radiation to get into an energetically more stable configuration. This form of radiation is divided into three different types of decays: α- and β-decay, as well as nuclear de-excitation (sometimes called γ-decay), which all differ in the way the nucleus loses energy.

In α-decays, the radioactive nucleus emits an α-particle consisting of two protons and two neutrons - identical to a helium nucleus. In β-decays, a proton (or a neutron) in the nucleus decays into a neturon, electron and electron-neutrino (or a proton, positron and electron-antineutrino respectively), with the latter two leaving the atom. The emitted electron (or positron) is also referred to as β-particle. In nuclear de-excitation, an excited nucleus decays into a lower energy state, emitting a gamma ray photon. This often happens after an α- or β-decay, which can leave the final nucleus in an excited state.

2.1.1 Beta decay

As the radioactive source used in the experiments for this thesis is 100% β-decaying, the process is discussed in more detail. There are two types of β-decay, depending on whether a nucleus contains an excess of neutrons or protons. In a neutron-rich nucleus, a neutron can transform into a proton via the process

$$n \to p + e^- + \bar{\nu}_e \,, \tag{2.1}$$

the so-called β^--decay. The electron and electron-antineutrino are emitted from the atom. The daughter nucleus now contains an extra proton, which means its atomic number is increased by 1.

Analogously nuclei with an abundance of protons can decay via

$$p \to n + e^+ + \nu_e \tag{2.2}$$

now transforming a proton into a neutron, emitting a positron and a neutrino. This is called β^+-decay and decreases the atomic number by 1.

As an alternative to β^+-decay, proton-rich nuclei may also transform themselves via the capture of an electron from one ot the atomic orbitals

$$p + e^- \to n + \nu_e \,. \tag{2.3}$$

This reaction is called electron capture and is essentially the same as β^+-decay but with the β-particle transposed to the left side and with the electron-neutrino being the only emitted particle [15].

Often the daughter nuclei are left in an excited state. They decay by nuclear de-excitation, emitting a gamma ray photon of characteristic energy level. The emittance of this photon, and hence previous radioactive decays, can easily be measured.

An example for a β-decaying source is the radioactive isotope of caesium ^{137}Cs, the source used in the experiments for this thesis. The decay scheme for ^{137}Cs is shown in figure 2.1. About 95% of all decays are β^--decays to the metastable nuclear isomer of barium $^{137\text{m}}$Ba, while the remaining 5% are directly to the stable ground state ^{137}Ba. $^{137\text{m}}$Ba has a half life of 2.552 min and decays to the ground state by emitting a 0.662 MeV gamma ray photon [19].

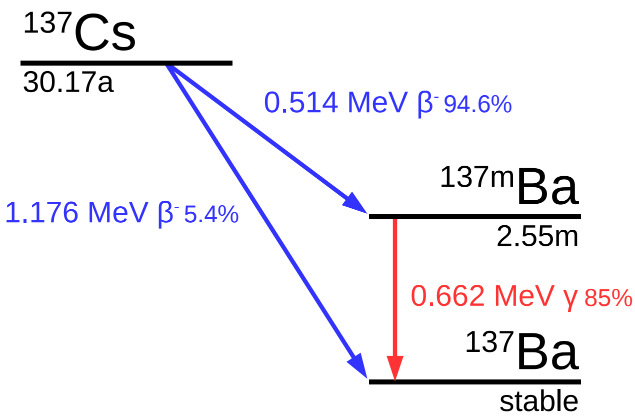

Figure 2.1: Decay scheme of ^{137}Cs [19].

2.1.2 Radioactive decay law

Radioactive decay - independent on its nature - can be described by a statistical process. Consider a source with N radioactive nuclei at time t. The decrease in number of nuclei over time is

$$dN = -\lambda N dt\,, \tag{2.4}$$

where λ is the decay constant, which is a property of the radioactive material. Integrating the previous equation leads to the number of nuclei as a function of time:

$$N(t) = N_0\, e^{-\lambda t}\,. \tag{2.5}$$

N_0 denotes the initial amount of radioactive nuclei at $t = 0$. This zero-point is arbitrary and does not have to correspond to the point in time at which the nucleus was created. The probability of a nucleus decaying at time t is always the same and does not depend on t_0.

The mean lifetime of a nucleus is

$$\tau = \frac{1}{\lambda} \tag{2.6}$$

and thus also a constant. It relates to the half-life

$$T_{\frac{1}{2}} = \tau\, \ln(2)\,, \tag{2.7}$$

which denotes the time required for the decaying quantity to fall to one half of its initial value.

The activity or decay rate of a radioactive source describes the number of decays per unit time:

$$A(t) = -\frac{dN}{dt} = \lambda N_0\, e^{-\lambda t} = \lambda\, N(t) = A_0\, e^{-\lambda t} \quad \text{with } A_0 = \lambda N_0\,. \tag{2.8}$$

It also follows the decay law (eq. (2.5)) and is proportional to the number of nuclei at time t. The SI derived unit for the activity of a source is the becquerel (Bq), which equals 1 decay/s [3].

2.2 Decay rate modulation

After the discovery of radioactivity and the establishment of the radioactive decay law, the question arised whether the decay constant λ could be influenced by external factors. In 1930 Rutherford, Chadwick and Ellis concluded that it is constant under all conditions [20]. This is nowadays widely accepted. However, in recent years different publications claimed to find evidence for the decay constant to vary with time.

2.2.1 Correlations between nuclear decay rates and Earth-Sun distance

In an article published in 2009, J. H. Jenkins et al. [13] report a strong correlation between unexplained periodic fluctuations in the decay rates of ^{32}Si and ^{226}Ra and the distance R between the Earth and the Sun. They analyzed data from an experiment at the Brookhaven National Laboratory (BNL), which measured the half-life of ^{32}Si with respect to a long-lived comparison source, in their case ^{36}Cl, between 1982 and 1986 [1]. To avoid systematic effects from the apparatus, the ratio $^{32}\mathrm{Si}/^{36}\mathrm{Cl} \equiv A(^{32}\mathrm{Si})/A(^{36}\mathrm{Cl})$ was computed and investigated. To compare results from experiments with different radioactive sources, Jenkins et al. studied the function $U(t) \equiv [A(t)/A(0)] \exp(+\lambda t)$, which is time-independent, e.g. normalized, for all nuclides. The result of their analysis is shown in figure 2.2 along with a plot of $1/R^2$. They claim that an annual modulation in the ^{32}Si/^{36}Cl ratio is clearly evident from the plot, with a probability of 6×10^{-18} that the correlation would arise from two uncorrelated data sets. The modulation amplitude of the ^{32}Si rate is approximately 0.15%.

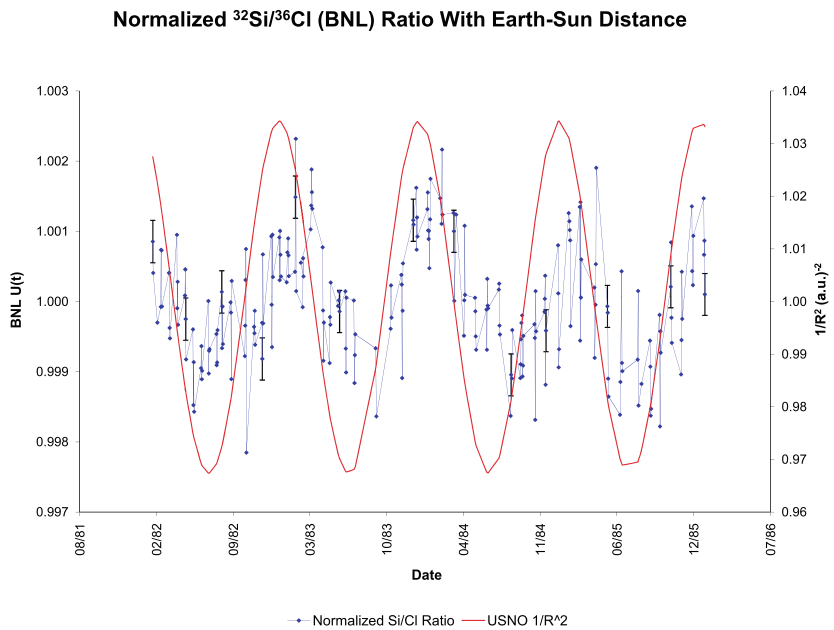

Figure 2.2: Plot of $U(t)$ for the raw BNL ^{32}Si/^{36}Cl ratio (blue) along with $1/R^2$ (red), where R is the Earth-Sun distance [13].

The data for ^{226}Ra are from an experiment performed at the Physikalisch-Technische Bundesanstalt (PTB) in Germany [21] and overlapped with the experiment at BNL for about two years. Jenkins et al. analyzed this data in the same way as for ^{32}Si and again claim to observe an annual modulation. Furthermore, they also suggest a correlation between both the BNL and PTB data with a probability of 4×10^{-12} that this arises from statistical fluctuations. Jenkins et al. mention the possibility of an interaction between nuclei on Earth and the neutrino flux from the Sun, which also varies with $1/R^2$, as a possible explanation for the observed modulations.

Another paper from Jenkins et al. in 2009 [12] is supporting this theory. They report a significant decrease in the decay rate of ^{54}Mn during a solar flare in December 2006. Dips in the measurement of the rate were coincidentally observed with X-rays from the solar flare, indicating a possible neutrino-influenced effect due to the change in solar activity during such a flare.

As a response to the propositions of a correlation between radioactive decay rates and the Earth-Sun distance, Norman et al. [18] from the University of California in Berkeley reexamined a large body of their collected decay data from 15 years, to search for periodic variations as seen by Jenkins et al. The experiment at Berkeley was designed to measure the half-lives of ^{44}Ti, $^{121\mathrm{m}}$Sn and $^{108\mathrm{m}}$Ag in separate gamma-ray experiments. To minimize influences of changes in detector and electronics reference isotopes were used for all experiments (namely ^{22}Na, ^{241}Am and ^{133}Ba). The observed ratios were corrected for the expected exponential decays of both isotopes in order to search for modulations. Statistical tests on both the null hypothesis (no annual variation) and the modulation hypothesis (variation in $1/R^2$ and amplitude of 0.15%) were performed. In all of the studied cases, the null hypothesis was strongly favored over the modulation hypothesis. The authors concluded, that there is no evidence for correlations between the Earth-Sun distance and the decay rates of the six studied isotopes. Further, they set limits on the possible modulation amplitudes 2.5-37 times smaller than observed by previous experiments [1],[21],[13].

2.2.2 Experimental results for different isotopes

If Jenkins et al. were right, this would have major consequences for various areas of science. Therefore different experiments took on the task of testing this proposal. Various radioactive sources have been tested for annual modulations over the past few years with different outcomes.

Beside the already discussed experiments, one dedicated modulation experiment was performed by Belotti et al. [4] in 2011 at the Gran Sasso National Underground Laboratory (LNGS) in Italy. They studied the activity of a ^{137}Cs source with a High-Purity Germanium detector. Due to the site's location deep underground the Gran Sasso massif, the flux of cosmic ray and neutron flux are reduced by factors 10^6 and 10^3 respectively [4]. The temperature was reported to be stable, with a maximum variation of 0.7 K. Data were collected continuously for 217 days. The activity of the source was calculated per 4 days giving the results shown in figure 2.3. The residual plot shows no modulation above or below 0.001%. Furthermore, the presence of time variations in the activity of the source larger than 9.6×10^{-5} could be excluded at 95% confidence level (C.L.), therefore rejecting the claim by Jenkins et al. [13].

In a paper following shortly after, Jenkins et al. [11] confirmed that they could not find any time variation in the decay rate of ^{137}Cs. However, they presented evidence of an annual modulation for ^{133}Ba. There are also other publications claiming to have found periodic fluctuations in the activity of radioactive sources, for example by Alexeyev et al. [2] for ^{214}Po and by Sturrock et al. [22] for the sources ^{108}Ag,

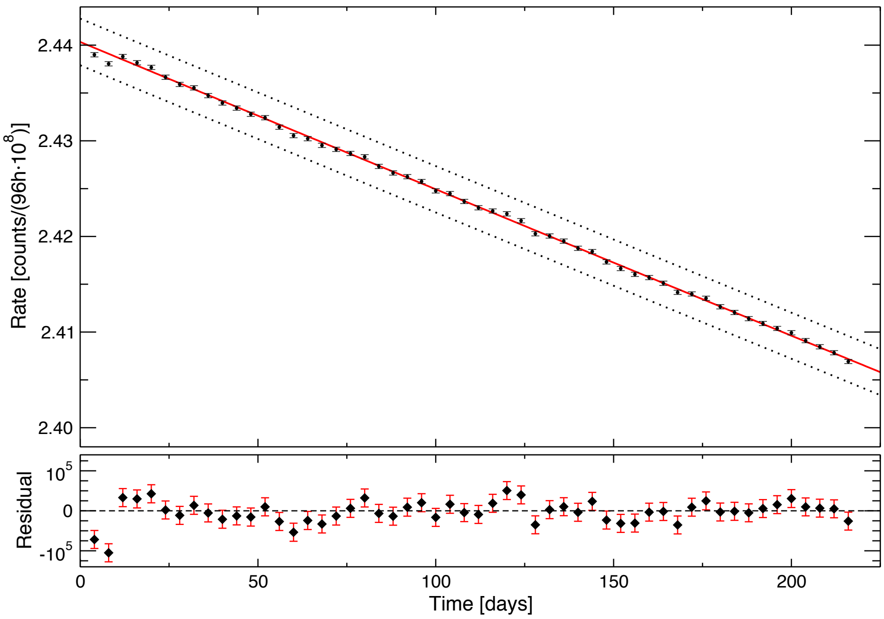

Figure 2.3: Experimental results for the detected activity of the ^{137}Cs source from the modulation experiment at LNGS. Dead-time corrected data are summed over 96 hours. The first two points correspond to the beginning of the data taking and were not considered in the analysis. The dotted lines are showing a 0.1% deviation from the exponential trend. Plotted below are the residuals of the measured activity to the exponential fit [4].

^{90}Sr, ^{152}Eu, ^{154}Eu, ^{226}Ra and ^{85}Kr. This list is not complete and shows that more experiments are needed to confirm or reject the claim by Jenkins et al. [13] about time-dependent decay constants.

2.2.3 Event rate modulation in direct dark matter search experiment

In 2008 Bernabei et al. [6] presented the first results of the DAMA/LIBRA experiment at LNGS, designed to directly detect dark matter (DM) particles in the galactic halo. As the Earth orbits around the Sun, the flux of DM particles from the galactic halo is not constant. In particular, the flux should be larger around June 2$^{\text{nd}}$, when the rotational velocity of the Earth is summed to the one of the solar system with respect to the Galaxy, and lower around December 2$^{\text{nd}}$, when the two velocities are opposite [7]. This means, that the measurement of events induced by DM particles in a suitable low background setup would show an annual modulation signature due to the Earth's revolution around the Sun.

DAMA/LIBRA exploits this signature by using highly radiopure NaI(Tl) scintillators as target-detectors for incoming DM particles. The obtained rates should follow a cosine function with a period of one year and a phase in June, while the modulation is only present in a well-defined low energy range, where DM particles can induce a signal. The experimental range for DAMA/LIBRA was 2-6 keV.

Combining the data of the preceding experiment DAMA/NaI with those from

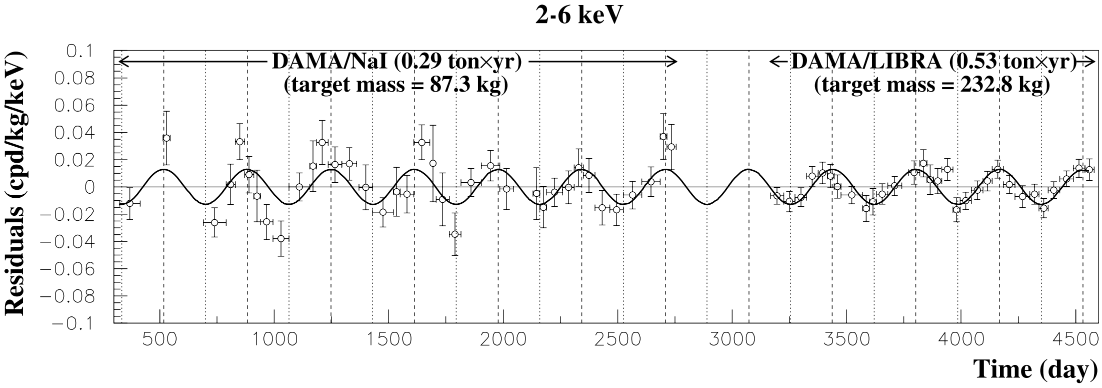

Figure 2.4: Residual rate of possible Dark Matter induced events measured by the DAMA/LIBRA and DAMA/NaI experiment in the 2-6 keV energy interval as a function of time. The superimposed curve represents a cosinusoidal function with a period of 1 year and a phase at June 2^{nd} with a modulation amplitude obtained by best fit over the whole data set [6].

DAMA/LIBRA, the authors state that the presence of DM particles in the galactic halo is supported on the basis of the annual modulation signature at a confidence level of $8.2\,\sigma$. The residual rate for the energy interval 2-6 keV is shown in figure 2.4 with the phase and period consistent to the expected values [6]. In a more recent paper by Bernabei et al. from 2013 [5] including a larger amount of data from DAMA/LIBRA, the C.L is given to be $9.3\,\sigma$ for the combined result from the two experimental setups.

Although Bernabei et al. claimed to have found evidence for the existence of DM particles in the galactic halo, no clear explanation for the observed signal was given. However, many publications rule out the possibility of the modulation signature originating from DM particles. For example XENON, another direct dark matter search experiment at LNGS, ruled out various DM models with electron interactions as the explanation of the observed modulations [24],[25]. Others tried to search for non-DM related explanations, like Klinger and Kudryavtsev from the University of Sheffield, which excluded muon-induced neutrons as a possible explanation of the DAMA/LIBRA data [14].

In a paper from 2013, Nistor et al. [17] consider the possibility that the observed annual modulation signature is induced by a contamination of potassium inside the detector used in the DAMA/LIBRA experiment. In contrast to the DM hypothesis, the annual signal could also arise from X-ray photons emitted in the detector itself from ^{40}K decays. The energy of such an X-ray photon is about 3.2 keV, inside the 2-6 keV range of the DAMA/LIBRA data. The authors also state the calculated ^{40}K event rate could account for the observed count rate in the experiment. However, this hypothesis strongly relies on the previously discussed suggestion by Jenkins et al. [13], that some nuclear decay rates exhibit an annual modulation due to solar influences. In order to verify this hypothesis, further studies on decay rate modulations need to be performed, such as in the modulation experiment discussed in the next chapter.

Chapter 3

The modulation experiment

The modulation experiment is a project which includes research groups from different geographical locations. Along the University of Zurich, scientists from the Dutch National Institute for Subatomic Physics Nikhef in Amsterdam, Purdue University in Indiana (USA), the Brazilian Center for Research in Physics in Rio de Janeiro and from the University of Freiburg (Germany) are part of the collaboration. The goal of the experiment is to measure if radioactive sources exhibit a yearly modulation in their activity of the order of 0.1% [8].

Various radioactive sources will be studied, to cover different energy ranges in the experiment. At UZH, the following three sources are observed: ^{60}Co (emitting gamma rays of 1173 and 1333 keV energy), ^{137}Cs (662 keV) and ^{44}Ti (68 and 78 keV). The modulation experiment is designed to save every single detector pulse, which gets time-stamped for later backtracking if a change in activity has been observed. Beside this, different external factors are monitored, e.g. temperature, humidity, radon levels and pressure. The experimental setup is identical at each of the four locations. By comparing the results, local influences can be excluded while effects that influence all setups simultaneously, such as interference from solar neutrinos, can be identified.

3.1 Experimental setup

The experimental setup is divided in an inner and outer box. The inner box contains the detectors and sources. Eight NaI(Tl) scintillation detectors viewed by PMTs are installed. Every source is monitored by a detector pair placed opposite of each other (see figure 3.1). One detector pair is used for background measurements. Every detector has a built-in light-emitting diode used to determine any change in PMT signal amplification over time. The inner box is air-tightly sealed and filled with radio-pure nitrogen gas to reduce the background influence of radon. Furthermore, the temperature is kept stable by placing two heat strips near the detectors. Various sensors measure environmental properties such as radon level, humidity, temperature and magnetic field inside the inner box. This data is saved for later backtracking.

To avoid influences from natural radioactivity the detector sets are enclosed by a lead shield.

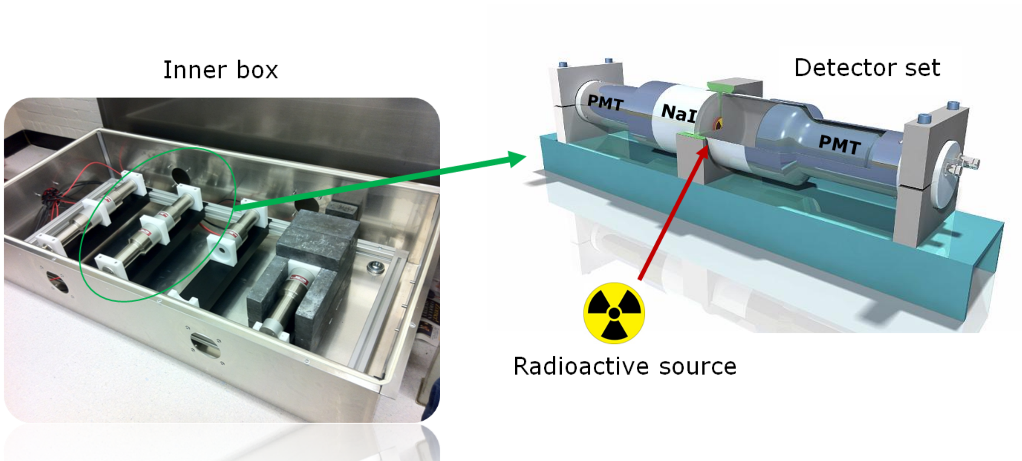

Figure 3.1: Left: Photo of the inner box with 7 NaI(Tl) detectors and one of the lead shields. Right: Drawing of one of the detector pairs with a radioactive source in between. Figure from [8].

The outer box contains the necessary electronics. The set of electronic devices contains

- high voltage supply for the detectors in the inner box
- NI-PXIe DAQ (Data Acquisition) with FPGA (Field Programmable Gate Array) module for data acquisition
- data storage server
- gas flow system, to flush the inner box with nitrogen
- radon meter, to monitor the level of natural radon in the box
- PID controller, which controls the temperature stability in the inner box. It also has a safety system which powers or shuts off the heaters if the temperature exceeds above or falls below the edges of the desired temperature range.
- LED circuit board, for signal shaping of LED test pulses (see section 4.1)

Connections to the outside of the experimental setup contain power supply, an Ethernet cable for data transfer to the computer and gas inflow.

On the computer a specifically designed LabView project called ModuDAQ is responsible for the data acquisition for the modulation experiment. Measurements can be started from the program and various parameters can be set. During a run, the status of the measurement can be monitored through the ModuDAQ. After successful data taking, the data has to be run through a processor, which converts the LabView files to readable ROOT files for further data analysis.

3.2 NaI(Tl) detectors

The detectors used in the modulation experiment are thallium-doped sodium iodide (NaI(Tl)) scintillation detectors. A schematic drawing of such a detector is shown in figure 3.2. It combines a scintillation crystal with a photomultiplier tube. The built-in LED is mounted next to the NaI(Tl) crystal to send a light pulse directly on the photocathode of the PMT. It has a diameter of 3 mm and emits light with a wavelength of 470 nm [8].

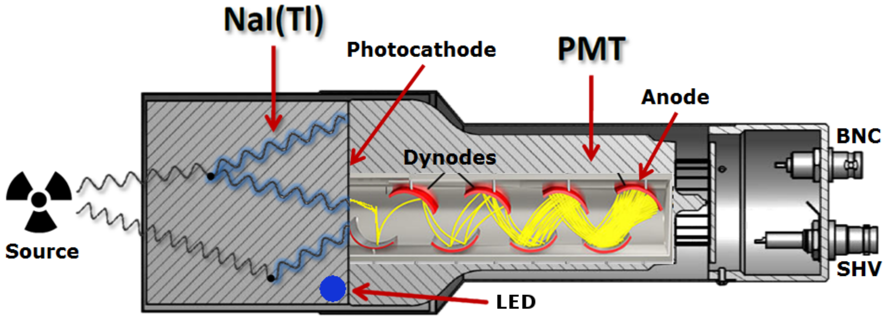

Figure 3.2: Schematic drawing of a detector, with the NaI(Tl) scintillation crystal, PMT and connectors (Image by K. Heijhoff, from [8]).

Scintillation detectors are among the most often used particle detection devices in nuclear and particle physics today. Certain materials, called scintillators, emit a small flash of light, a scintillation, when struck by radiation. With an amplifying device such as a PMT, this light is converted into electrical pulses, which can be analyzed and counted.

Scintillation detectors have two main features. First, they have a near linear response to the deposited energy, which means that the light output of a scintillator is directly proportional to the excitation energy. In connection with a PMT, also a linear device, the final signal will be proportional to the energy of the incident particle, making scintillation detectors suitable as an energy spectrometer. Second, their response and recovery time are short in relation to other particle detectors. This allows higher counting rates due to shorter deadtime.

When radiation passes through a scintillating material, the material absorbs and re-emits the energy in form of light. This effect is called *luminescence* and has two forms: *fluorescence*, if the reemission of the energy happens immediately after the absorption (within 10^{-8} s), and *phosphorescence* or *afterglow*, if the reemission is delayed. In the latter case the delay time can be anywhere between a few microseconds to hours depending on the material. This effect has to be taken into account when dealing with high event rates.

There are different types of scintillating materials in use, among them are inorganic crystals. These are often alkali metal halides containing impurity or activator atoms, such as NaI(Tl). In general, an incoming nuclear particle can ionize an atom in the crystal and create an electron-hole pair, which moves freely through the crystal. The impurity atoms can be excited by these electron-hole pairs and de-excite afterwards by emitting photons, which travel through the crystal and are registered as luminescence.

The main disadvantage of inorganic crystals is hygroscopicity, i.e. they easily attract water from their surroundings. Therefore, they must be housed in a sealed enclosure. Inorganic crystals are also not the fastest scintillation detectors, the decay constant for the energy reemission of NaI(Tl) is 230 ns. However, they have a great stopping power due to high densities ($\rho_{\mathrm{NaI(Tl)}} = 3.67\,\mathrm{g/cm^3}$) and atomic numbers, meaning they convert most of the incoming radiation to scintillation light. As they also have a very high light output (for NaI(Tl): 230% compared to reference light output of anthracene) resulting in a better energy resolution, inorganic crystals are extremely suitable for the detection of gamma ray photons, as needed by the modulation experiment [15].

Because the intensity of the emitted light is low, the signal has to be amplified in order to be counted. This can be done by using photomultiplier tubes. The main parts of a PMT are sketched in figure 3.2. It consists of a photocathode, an electron multiplier section with several dynodes and an anode, from which the signal can be readout. A high voltage potential (bias) is applied between these parts.

An incoming photon strikes the photocathode, which is made out of a material with a low work function resulting in a high probability for an electron to be emitted via the photoelectric effect. The applied voltage difference directs and accelerates the electron towards the first dynode. By hitting it, the incident electron transfers energy to the electrons in the dynode. This causes secondary electrons to be emitted, which again are accelerated towards the next dynode creating further secondary electrons. A so-called electron cascade is created, with an *electron amplification factor* or *gain* in the range of 10^4 to 10^7 [9], mostly depending on the number of dynodes in the PMT. The electron cascade arriving at the anode induces a current which can be amplified and analyzed. The PMT used in the detectors for the modulation experiment have 10 high gain, high stability dynodes, resulting in a gain of 7×10^5 at $850\,\mathrm{V}$ [8].

Another relevant quantity is the ratio of the number of created photoelectrons and the number of incident photons, called the *quantum efficiency* of the photocathode. It depends on the wavelength of the incoming light and determines the photon conversion efficiency. For the PMT used in the modulation experiment, the wavelength at maximum emission for NaI(Tl) ($\lambda = 415\,\mathrm{nm}$) is in the region of highest quantum efficiency, namely around 25 to 30% [8].

Chapter 4

Functionality test of built-in LEDs

The built-in LEDs in the NaI(Tl) detectors serve for PMT gain calibration and as an indicator for change in PMT signal amplification, and dead time calibration. These LEDs can send out test pulses, which are controlled by the ModuDAQ. During the final long-term run, the test pulses will be sent out in equally spaced time intervals. Observing the PMT response to these test pulses gives hints about possible changes in signal amplification, as the expected LED signal should not change over time. Additionally, the test pulses can be used to calibrate the system dead time by comparing the number of sent pulses to the number of pulses detected by the PMT. The work for this thesis consisted of setting up the electronics and checking the detection efficiency of the test pulses.

4.1 Setup and electronics

As already mentioned, all the LED test pulse setting are controlled via a special LED pulser panel in the ModuDAQ. The width of a pulse and the separation between two pulses can be adjusted. The digital output of a digitizer sends square waves to an electric circuit (shown in figure 4.1). When the transistor sees a rising edge from the incoming square wave, it immediately turns on using the 5 V power supply. The capacitor and resistance form a RC-circuit and shape the processed signal to have a falling edge (as seen in figure 4.3). The main idea is to shape the digital signal to an output signal similar to that of a detected photon. The LED circuit board has been designed and assembled at Nikhef in Amsterdam. Figure 4.2 shows a picture of the soldered circuit board.

The signal is then transmitted to the LED, which sends out a light pulse accordingly. This test pulse is detected by the PMT and processed in the same ways as normal data. The data acquisition is designed to flag LED pulses for distinction between LED- and source- or background-induced pulses. This is done by bit-manipulation of the 14-bit long raw voltage data, which is stored as a 16-bit integer and thus has 2 unused bits at the end. These will be overwritten in case of an LED test pulse and give additional information on the nature of the detected signal.

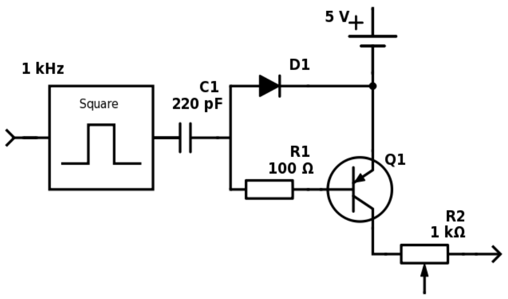

Figure 4.1: Schematic diagram of the electric circuit

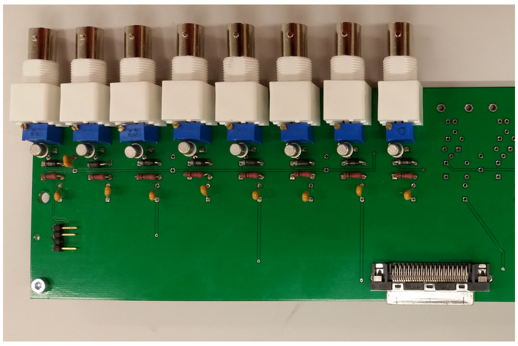

Figure 4.2: A picture of the LED circuit board.

To check the circuit response, an oscilloscope was used to view the signal shapes for every detector. Figure 4.3 shows the observed signals for all channels. All signals have the desired falling edge, although two of the channels (LED 1 and LED 5) show a slightly different response. A possible transistor defect was ruled out by exchanging the original parts with new ones, while the shape did not change. After several check-ups, the origin of the effect remained unclear. The decision was made to go on with the intended measurements. There was no observed difference during the measurements between the two channels and the others, hence a slightly different shape of the circuit response does not affect the LED test pulse as long as it has a falling edge.

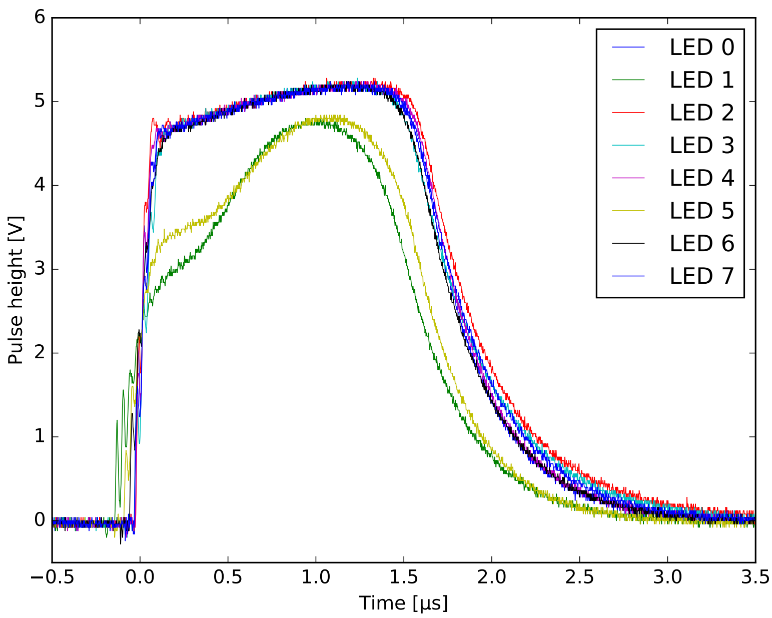

Figure 4.3: Circuit board response observed by an oscilloscope for all eight LEDs.

4.2 Background measurements

A first measurement was performed with all detectors on but no sources placed between them, i.e. only background events were observed apart from LED test pulses. The LED pulser was set to a frequency of 1 kHz, so there should have been a pulse sent every 1 ms. To verify this, the time between two subsequent LED-tagged events was calculated and plotted. This is shown in figure 4.4 for channel 6, while the plots for all the other channels look similar. There are three clear peaks, with the highest being at a time separation of 1 ms as expected for the 1 kHz pulse rate. A small peak at double the time difference (2 ms) indicates that few LED events were skipped during event tagging. In the presented channel, there are two skipped LED events. Compared to the total 555'334 recorded LED events, this effect is negligible. There are also some events tagged as overlapping (0 ms time difference), which may result from a mix-up with a background event detected at the same time as an LED event.

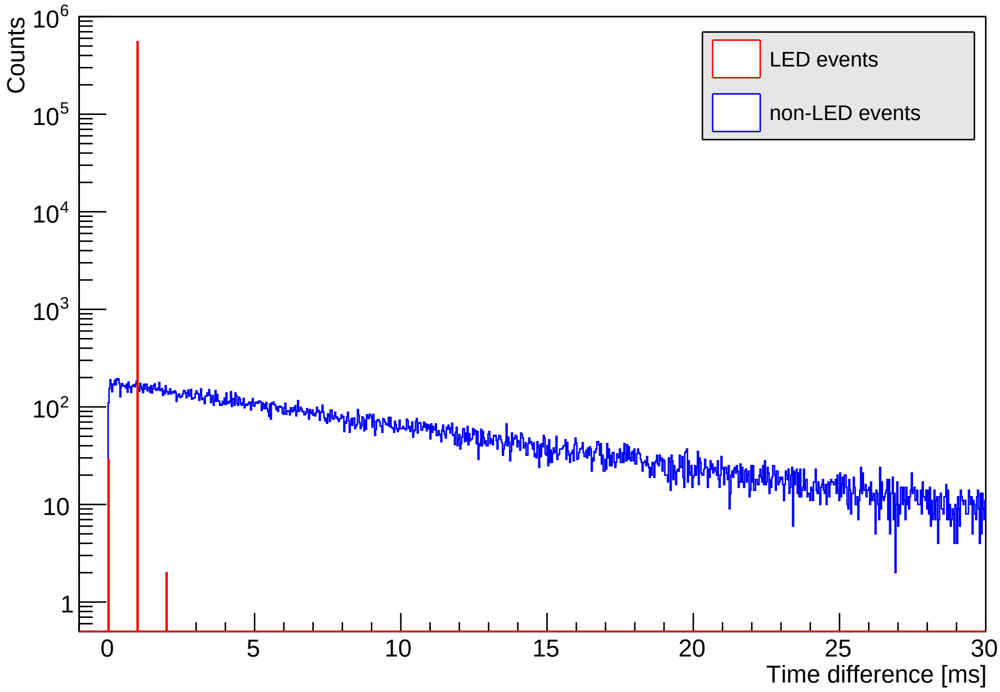

Figure 4.4: Time between two subsequent events for LED-tagged (red) and background-tagged (blue) events for channel 6.

Data was acquired for 555.30 s. With a pulse rate of 1 kHz a total number of 555'300 LED events should have been observed. Table 4.1 shows the measured number of LED events for each channel along with the number of observed background events. Overall, the number of measured LED events exceeded the expected number of LED events by 331, indicating that some background events are falsely flagged as LED events when they are detected sufficiently close to a real LED event. This would also explain the presence of the first peak at zero time difference in figure 4.4. However, compared with the total number of expected LED events (4’442’400), this excess is insignificant. Hence the detection and tagging of test pulses works as intended.

Table 4.1: Results for the measurement of LED-tagging with no source placed in the detectors. The duration of data taking was 555.30 s for every detector.

#	expected LED events	observed LED events	observed background events
0	555’300	555’356	78’284
1	555’300	555’362	81’349
2	555’300	555’331	52’594
3	555’300	555’337	51’098
4	555’300	555’331	52’553
5	555’300	555’332	51’787
6	555’300	555’334	56’272
7	555’300	555’348	52’413

4.3 Measurements with sources

In the configuration of the long-term run, the LED pulses will be detected along with gamma rays from the monitored radioactive sources. Therefore, a second measurement was done with the ^{137}Cs source placed between the detectors as a reference sample. Again the time between two subsequent events has been calculated for LED and particle events. An example plot is shown in figure 4.5. Compared to the plot where no source was monitored (figure 4.4) the absence of the skipped LED peak can be noted, which is the same for all the detectors. The peak at time difference 1 ms is still the highest. The increased number of overlapping LED events can be explained by a longer time of data taking and a higher activity of the ^{137}Cs source compared to background-only events and therefore a higher chance of an LED and particle event being detected close to each other.

The origin of the non-LED events are the photons emitted by the gamma decay in the follow-up of the beta decay of ^{137}Cs and background photons. Since gamma decay is a Poisson process, the time between two subsequently emitted gamma rays follows a decaying exponential function. This can be seen clearly in figure 4.5.

Table 4.2 shows the duration of the runs for each detector along with the expected number of LED events for a pulse rate of 1 kHz, the number and rate of measured LED events, and the number of observed particle-tagged events. The observed rate is higher for all detectors than expected, however the deviation is negligible and due to the fact of overlapping LED and source events.

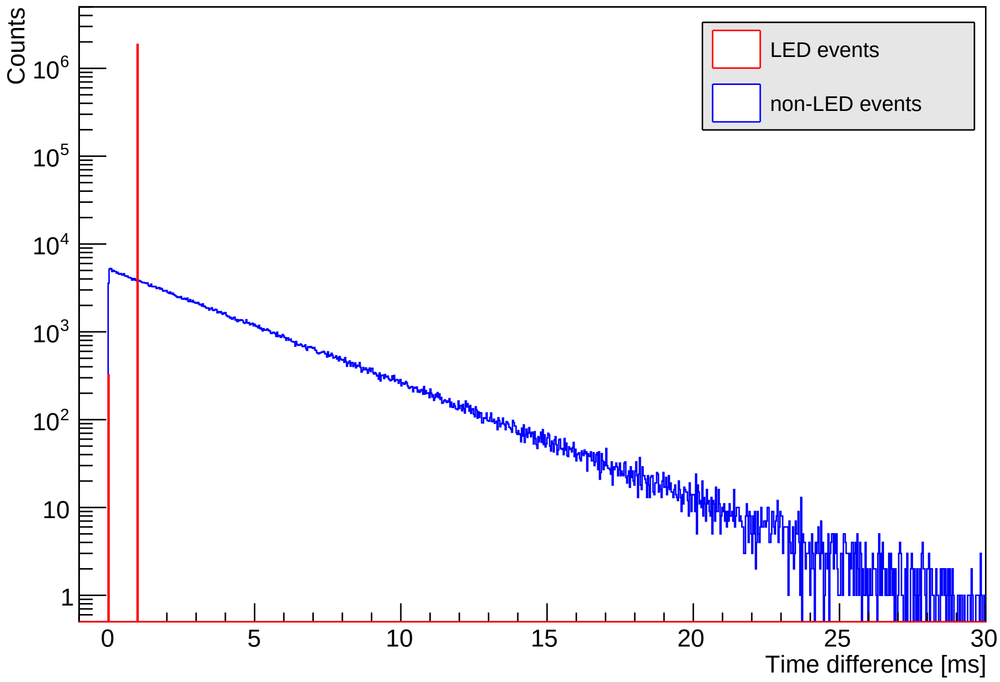

Figure 4.5: Time between two subsequent events for LED-tagged (red) and non-LED-tagged (blue) events for channel 6.

Table 4.2: Results for the measurement of LED-tagging with ^{137}Cs in the setup. Two detectors were run together at a time.

#	time [s]	expected LED events	observed LED events	observed rate [Hz]	observed non-LED events
0	1814.69	1'814'690	1'815'060	1000.20	571'895
1	1814.69	1'814'690	1'815'106	1000.23	698'120
2	1891.35	1'891'350	1'891'642	1000.15	515'771
3	1891.35	1'891'350	1'891'714	1000.19	565'729
4	1812.27	1'812'270	1'812'642	1000.20	536'335
5	1812.27	1'812'270	1'812'674	1000.22	641'032
6	1872.56	1'872'560	1'872'883	1000.18	560'732
7	1872.56	1'872'560	1'872'933	1000.20	613'321

Chapter 5

Study of decay rate behaviour as a function of pressure

Various external factors, such as temperature, cosmic radiation or radon level, could influence the measurements of radioactive sources. Another varying environmental parameter to consider is pressure. A pressure sensor will monitor the level of pressure inside the inner box once the long-term experiment is running. Since the modulation experiment aims at observing modulations with an amplitude of about 0.1%, the sensitivity of the measurement must be at least as accurate as this. To make sure that fluctuations in pressure do not affect the decay rate measurements at a higher level, the detectors had to be tested on how the observed rate changed while pressure was varied.

5.1 Setup and measurement procedure

Because the modulation box was not suitable to perform studies with variations in pressure, the measurements had to be done in an external setup. A cylindrical steel vessel from a previous experiment at UZH was used to house one of the NaI(Tl) detectors and the radioactive source ^{137}Cs. The chamber was high enough to allow the detector to stand on top of the source, making use of gravity to keep it in place. A vacuum pump was used to pump the air out of the chamber, which was afterwards flushed with nitrogen gas to establish different levels of pressure. The connections for high voltage, signal, pressure sensor, vacuum pump and gas supply were done with suitable feedthroughs at the flange of the chamber. Figure 5.1 shows the open vessel with the standing detector inside on the left, and the flange with all the feedthroughs on the right. To reduce background radiation, lead bricks were used to shield the vessel as seen in figure 5.2.

Once the setup had been completed, the air inside the chamber was pumped out and the level of pressure could be changed by flushing it with nitrogen gas. The measurements were performed in steps of 0.1 bar. A first set of measurements was always obtained while *increasing pressure* and a second one while *decreasing pressure*

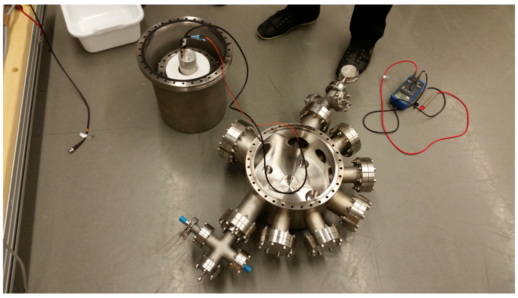

Figure 5.1: Open vessel for the pressure measurements (left) with flange (right).

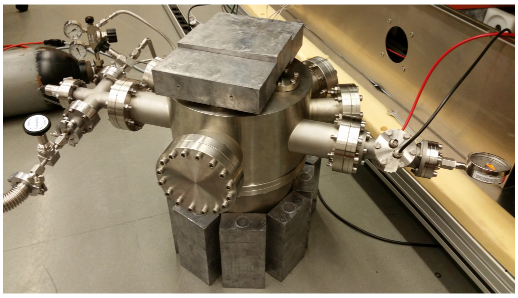

Figure 5.2: Closed vessel with lead shielding

inside the vessel. This was done in order to quantify the systematic errors.

After finishing a measurement run, the observed energy spectrum was analyzed by fitting a Gaussian to the photopeak (see figure 5.3) using a built-in fit function of ROOT. Initial parameters were 662 keV for the mean and 30 keV for the sigma. After obtaining the fitted parameters, the number of events with a measured energy within a 2σ range around the fitted mean was counted. This number was then divided by the total acquisition time to get an estimate of the rate in the photopeak range. This procedure was applied to all obtained energy spectra.

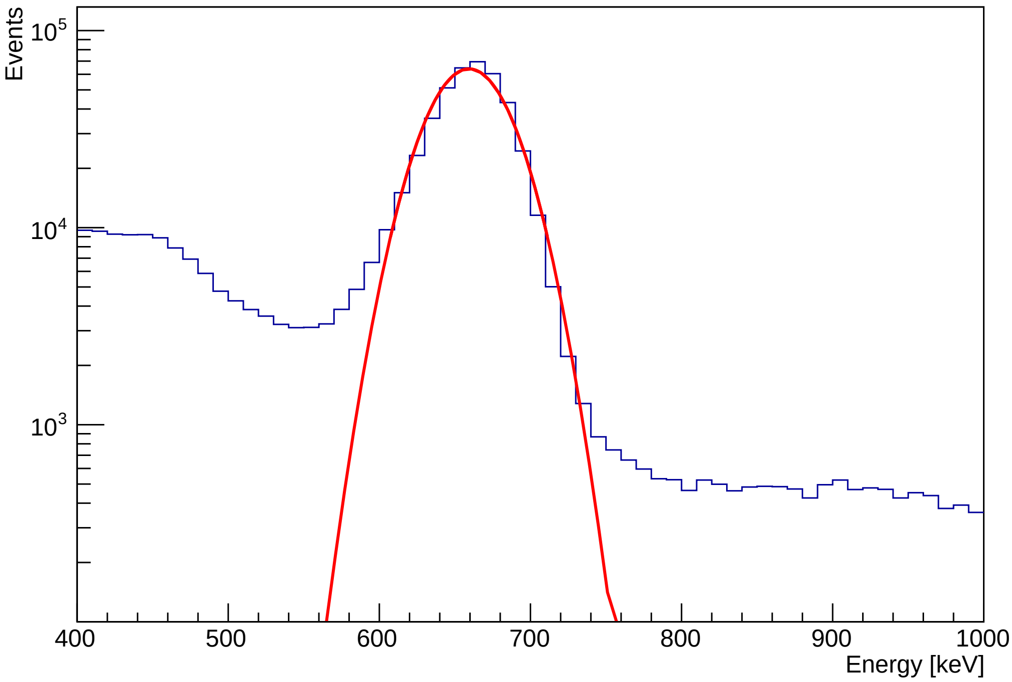

Figure 5.3: Gaussian fit (red) to the photopeak of ^{137}Cs of the acquired energy spectrum (blue) at 1.499 ± 0.002 bar in the first run, with a mean at 659.5 keV and a σ of 26.3 keV

Figure 5.4 shows the obtained fit values for mean (data point) and sigma (error bar) for the first run data set with increasing pressure. Two things can be noted. The mean does not move within the data set and the sigmas also agree. This is true for all measurement runs. However, the obtained values for the mean ($\approx 659.5\,\mathrm{keV}$) are smaller than the expected value (photopeak at 662 keV). This is attributed to the contribution of the tail of the compton edge, which is higher at the lower edge of the photopeak, hence the mean of the Gaussian fit gets shifted towards a lower value.

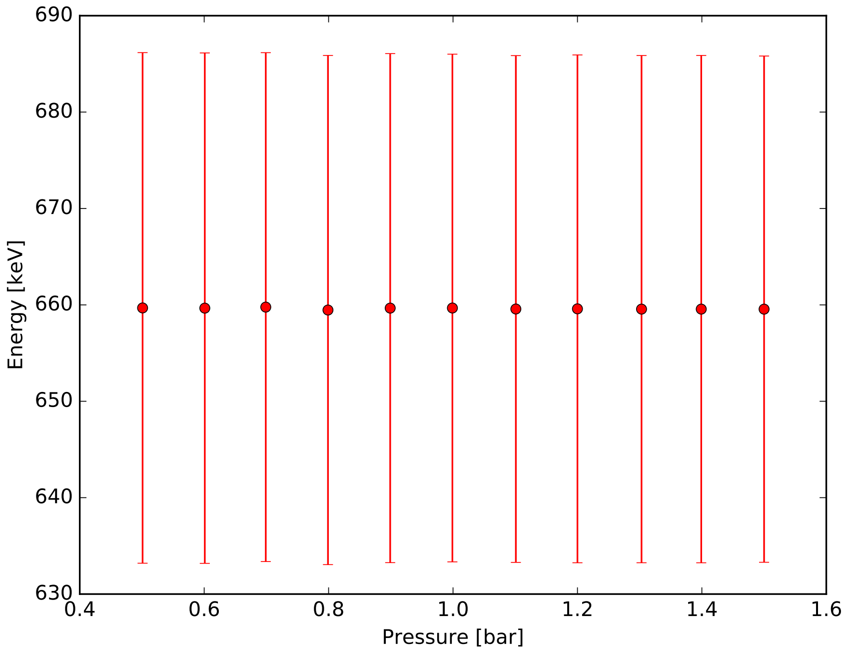

Figure 5.4: Fitted mean and sigma for each pressure setting for the increasing pressure data set from the first run. Data points are the mean with the error bars depicting the obtained value for sigma.

5.2 Measurements with 1 hour data acquisition

The first set of measurements was obtained by using the detector with the serial number SBL262 and the ^{137}Cs source. Pressure was varied between 0.5 and 1.5 bar and at every level data were acquired for 1 hour. It was expected that the decay rate is independent on the pressure inside the chamber and should therefore stay stable within statistical errors.

Following the radioactive decay law (section 2.1.2), the decay rate of a source decreases exponentially with time (eq. (2.8)). The obtained rate should therefore be normalized to the initial activity. The duration of the measurement was about 70 hours. After this amount of time, the activity of a ^{137}Cs source should have dropped by 0.02% according to its half-life value, which is stated to be $11'018 \pm 9.5$ days (30.17 ± 0.03 years) by the National Institute of Standards and Technology [16]. The relative error on the measured rate at the last data point is 0.2%, one magnitude larger than the expected activity drop. Therefore it was assumed that the exponential correction is negligible.

The observed rates for the first set of measurements are shown in figure 5.5. There seems to be a dependency on pressure for values below 0.9 bar. The rise in rate while increasing pressure is confirmed by a drop in rate while decreasing pressure, so the observed effect is independent on the direction of the pressure change.

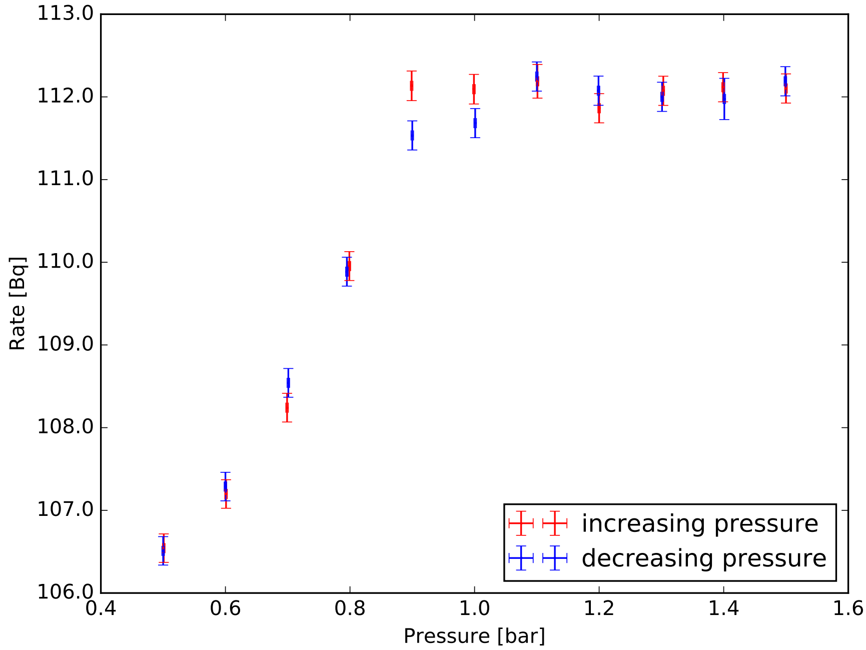

Figure 5.5: Measured activity of the source as a function of pressure with 1 hour data acquisition at every point. Errors on the rate are statistical, pressure values have a systematical error of ± 0.002 bar.

To explore the origins of the observed rise/fall of decay rates at lower pressure levels in the first run, another 1 hour measurement was performed with a different detector (serial number SBL259) to rule out that the effect originates from a specific detector. Still monitoring the ^{137}Cs source, rates were obtained at increasing and decreasing pressure levels. The result is shown in figure 5.6. The same effect as in run 1 can be observed. This indicates that either the effect is of pure physical nature, e.g. of the source itself, or it is a feature of the detectors or the setup in general.

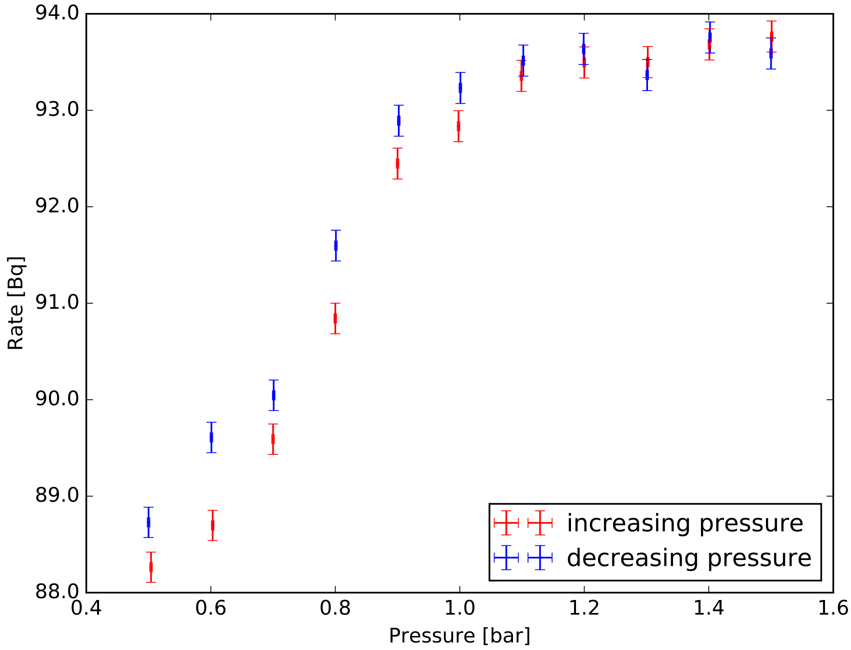

Figure 5.6: Measured decay rates versus pressure level for the second 1 hour run.

5.3 Measurements with 8 hours data acquisition

To explore this behaviour in a range of pressure fluctuations closer to the conditions expected during the long-term run, the measurement was repeated on a smaller pressure range from 0.9 bar to 1.1 bar in steps of 0.05 bar. The experiment run for approximately 8 hours at each pressure level to increase statistics. The calculated decay rates are plotted in figure 5.7. Only a slight rising trend is identifiable, but the results for 1.0, 1.05 and 1.1 bar agree for in- and decreasing pressure.

A relative residual plot should give a good indication about the order of the observed fluctuations. The mean decay rate was calculated and used as the reference point. Figure 5.8 shows the relative residual for each data point. The highlighted area marks the region, where the fluctuations are less than 0.1% of the mean rate, the sensitivity required by the modulation experiment. The plot shows, that the observed decay rates are in or near this sensitivity area, but in general the fluctuations are higher than what the experiment is aiming at. The root mean square (RMS) error was calculated to be 0.12%.

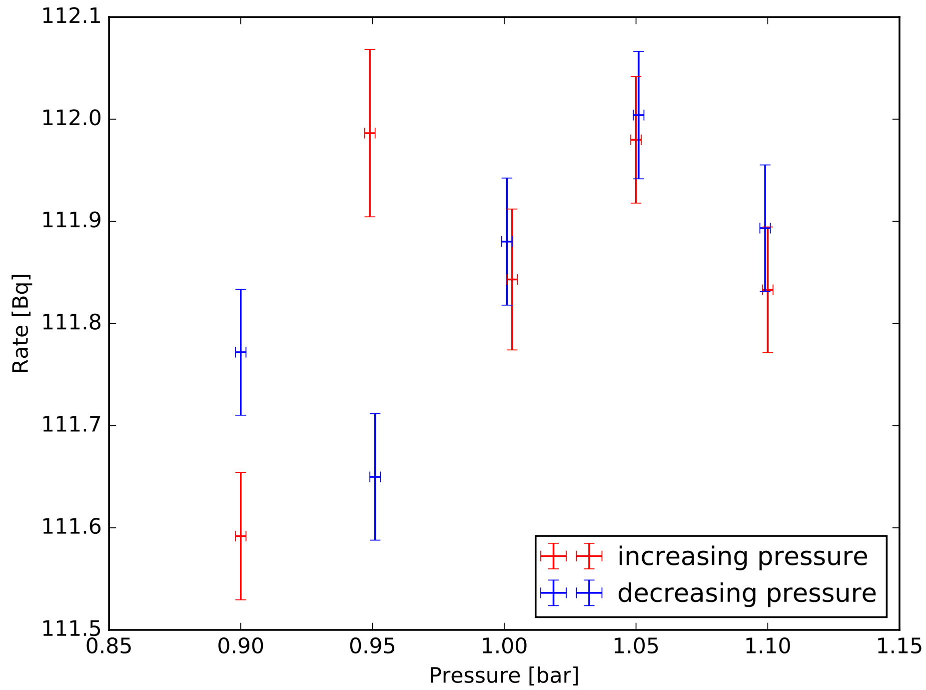

Figure 5.7: Measured decay rates as a function of pressure with 8 hours data acquisition time at each pressure setting.

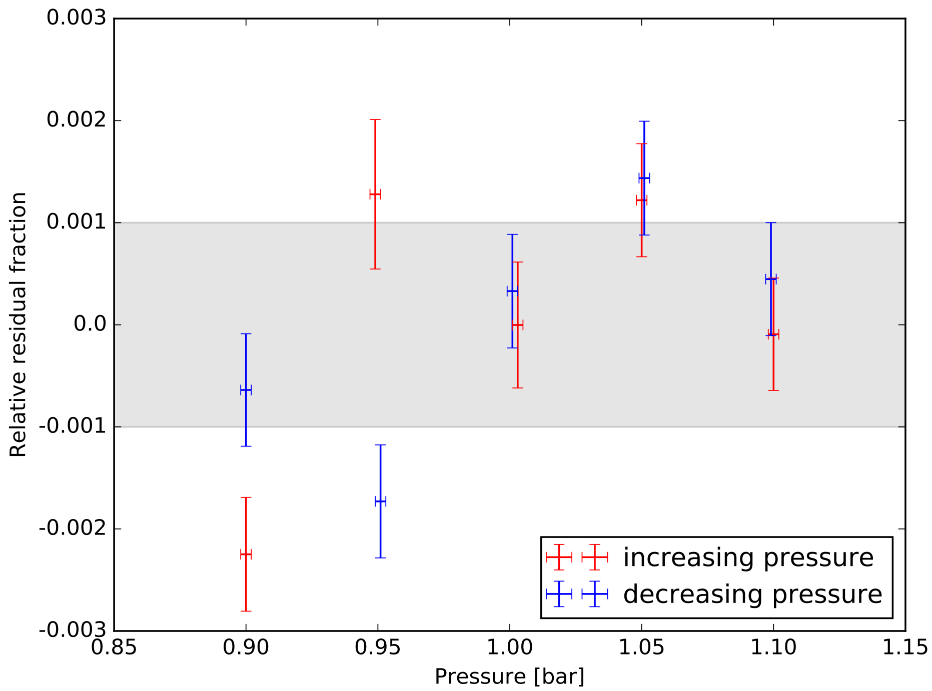

Figure 5.8: Residuals of the obtained decay rates relative to the mean rate $111.8 \pm 0.1\,\mathrm{Bq}$.

5.4 Spectral analysis

A closer look at the obtained energy spectra was taken to search for the cause of the observed effects. The measurements used were the data collected for the second run with 1 hour acquisition time at decreasing pressure (see the plot in figure 5.6 for reference). All the energy spectra for the different pressure levels were compared to the one obtained at 1.5 bar. The upper plot in figure 5.9 shows the spectrum obtained at 0.5 bar and the reference spectrum at 1.5 bar. The number of events in each energy histogram bin was subtracted from the reference spectrum and then divided by the number of events in the energy histogram bin of the reference spectrum. This gives a relative difference histogram for every energy bin. This relative difference plot for the two already mentioned spectra is shown in the lower plot in figure 5.9.

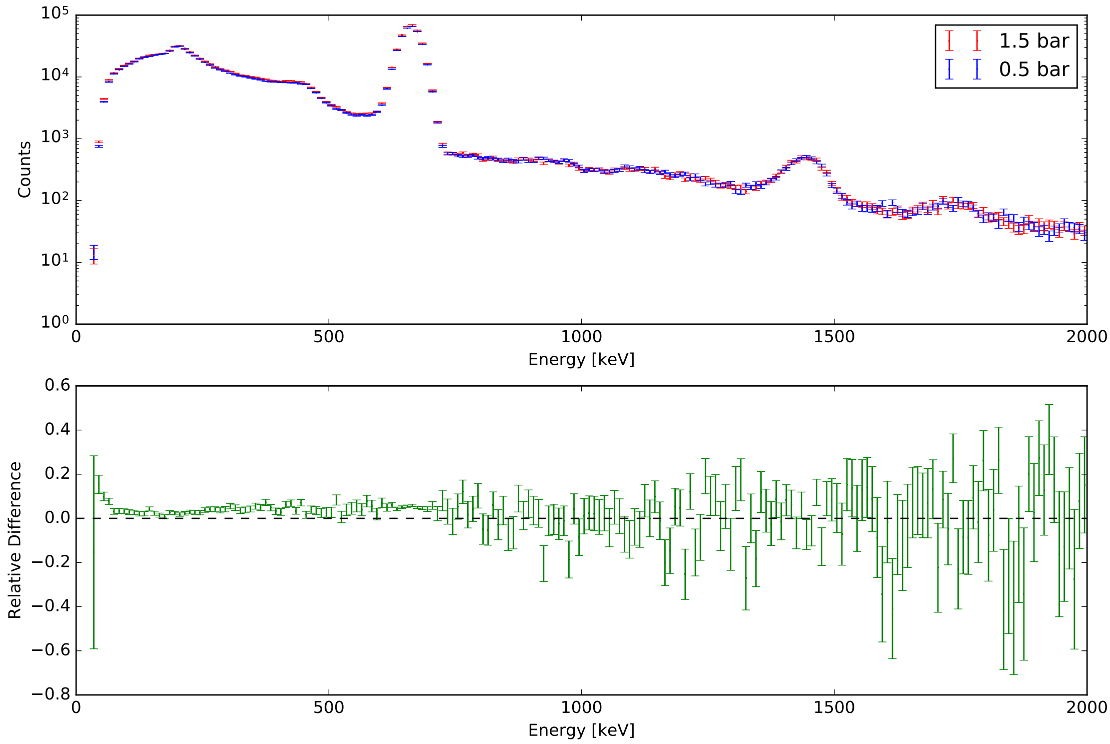

Figure 5.9: Above: Obtained energy spectra for the data set at 0.5 bar (blue) and the reference data set at 1.5 bar (red). Below: Relative difference between the two spectra.

Three effects can be observed. First, there is a major difference in number of events at energies near the threshold energy, which was observed to be around 38 keV, but was not changed during the course of the measurements. Second, there are generally more events below the upper edge of the photopeak, where the gamma rays from the source dominate the spectrum. Finally, at energies above the photopeak energy, where there should only be background related photons, the difference is just a statistical fluctuation, as expected.

Furthermore, the total number of recorded events in different energy regions were compared for every pressure measurement. The compared energy regions were

1. 0 - 2000 keV, the total measured energy range
2. 0 - 600 keV, energy range below the photopeak
3. 600 - 720 keV, energy range around the photopeak
4. 720 - 2000 keV, energy range above the photopeak, where background-induced events should dominate

The number of events in every region was again computed relative to the reference spectrum at 1.5 bar. The results are shown in figure 5.10. In all ranges containing data from source events (1.-3.), the relative number of events follows a similar trend as in the plot of the decay rates (fig. 5.6), indicating that the observed raise/fall effect originates from the source itself. This is supported by the numbers from the background energy range, which are all comparable to the number from the reference source, hence not depending on pressure variations.

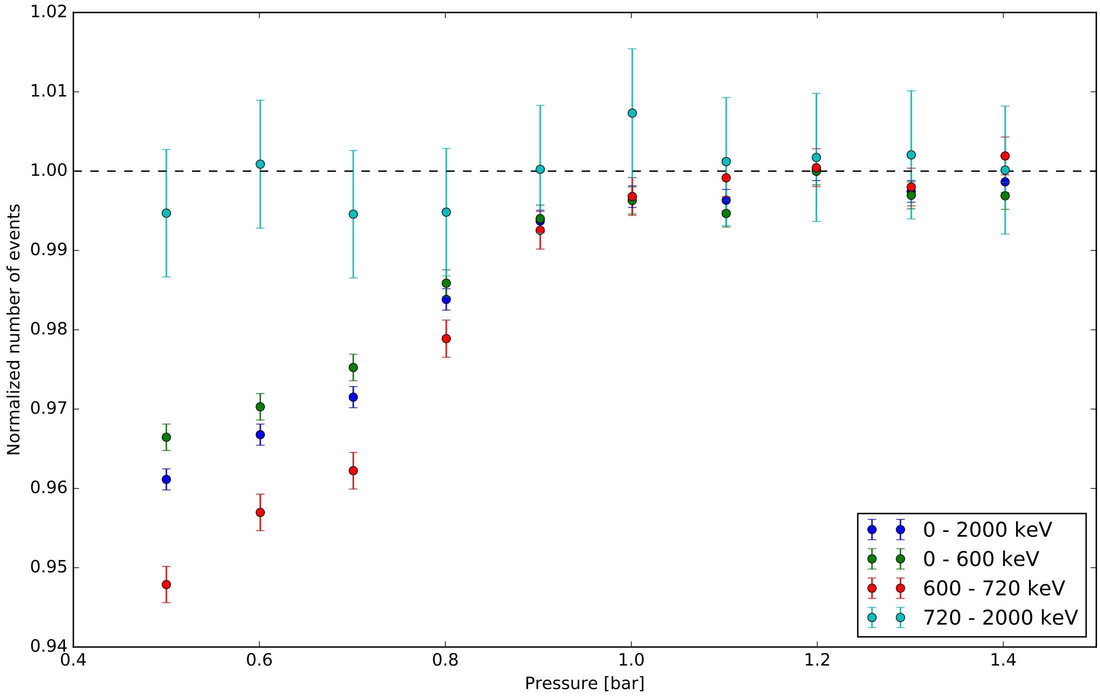

Figure 5.10: Comparison of the normalized number of events in different energy ranges for spectra obtained at every pressure level, with respect to the reference spectrum at 1.5 bar.

Chapter 6

Discussion and Conclusion

The measurements performed within the scope of this thesis were assigned to the two following tasks:

1. Exploring the functionality of the LED test pulse tagging

Although the response of the electric circuit showed irregularities for two of the eight channels, this had no effect on the functionality. The results of the measurements show that the distinction between the LED test pulses and a real photon signal by bit-manipulating of the processed data is working as expected with few photon signals mistagged as LED events when detected too close to each other. In the case of a source monitored by the detector, the observed rate of the LED test pulses is insignificantly higher than expected by $(0.0196 \pm 0.0009)\%$.

2. Investigating the sensitivity of the detectors to pressure fluctuations

The results of the first two measurements with 1 hour data acquisition time at every pressure level in the range 0.5 to 1.5 bar shows a rise/fall of the measured decay rates below 0.9 bar. Because the expected pressure fluctuations in the final modulation experiment are not this large, the measurement was repeated in a smaller pressure range with 8 hours of data acquisition time. The rise/fall effect was not seen, but the decay rate variations are at or above the desired limit of 0.1%, with an RMS value of 0.12%.

In order to search for the cause of the rise/fall effect in the first two runs, the obtained energy spectra were analyzed. The results indicate that the effect is source-related and does not originate from background effects. However, the true nature of the effect could not be explained. Besides the unlikely explanation that the pressure affects the activity of the source directly, it is more probable that the experimental conditions changed with pressure variations. A possible explanation could be that the distance between source and detector changes due to the detector material being affected by varying pressure. This would result in a lower observed source activity [8], while the background stays stable.

In general, there was an observable effect of pressure variations on the measured rate. This needs to be accounted for in future measurements, either by deconvolution or a second, more detailed study on pressure variations at operational conditions.

References

[1] D. E. Alburger, G. Harbottle, and E. F. Norton. Half-life of ^{32}Si. *Earth and Planetary Science Letters*, 78(2-3):168–176, 1986.

[2] E. N. Alexeyev, Y. M. Gavrilyuk, A. M. Gangapshev, V. V. Kazalov, V. V. Kuzminov, S. I. Panasenko, and S. S. Ratkevich. Results of a search for daily and annual variations of the ^{214}Po half-life at the two year observation period. *Physics of Particles and Nuclei*, 47(6):986–994, 2016.

[3] C. Amsler. *Kern- und Teilchenphysik*. vdf Hochschulverlag AG, 2007.

[4] E. Bellotti, C. Broggini, G. Di Carlo, M. Laubenstein, and R. Menegazzo. Search for time dependence of the ^{137}Cs decay constant. *Physics Letters B*, 710(1):114–117, 2012.

[5] R. Bernabei, P. Belli, F. Cappella, V. Caracciolo, S. Castellano, R. Cerulli, C. J. Dai, A. d'Angelo, S. d'Angelo, A. Di Marco, H. L. He, A. Incicchitti, H. H. Kuang, X. H. Ma, F. Montecchia, D. Prosperi, X. D. Sheng, R. G. Wang, and Z. P. Ye. Final model independent result of DAMA/LIBRA–phase1. *The European Physical Journal C*, 73(12):2648, 2013.

[6] R. Bernabei, P. Belli, F. Cappella, R. Cerulli, C. J. Dai, A. d'Angelo, H. L. He, A. Incicchitti, H. H. Kuang, J. M. Ma, F. Montecchia, F. Nozzoli, D. Prosperi, X. D. Sheng, and Z. P. Ye. First results from DAMA/LIBRA and the combined results with DAMA/NaI. *The European Physical Journal C*, 56(3):333–355, 2008.

[7] R. Bernabei, P. Belli, F. Cappella, R. Cerulli, F. Montechia, F. Nozzoli, A. Incicchitti, D. Prosperi, C. Dai, H. Kuang, J. Ma, and Z. Ye. Dark Matter Search. *La Rivista del Nuovo Cimento*, 26(1):1–73, 2003.

[8] S. Breur. The performance of NaI(Tl) scintillation detectors. Master Thesis, University of Amsterdam, 2013.

[9] A. Das and T. Ferbel. *Introduction to Nuclear and Particle Physics*. World Scientific Publishing Company, 2003.

[10] H. Friedmann. *Einführung in die Kernphysik*. Wiley-VCH Verlag GmbH, 2014.

[11] J. Jenkins, E. Fischbach, D. Javorsek II, R. Lee, and P. Sturrock. Concerning the time dependence of the decay rate of ^{137}Cs. *Applied Radiation and Isotopes*, 74:50–55, 2013.

[12] J. H. Jenkins and E. Fischbach. Perturbation of nuclear decay rates during the solar flare of 2006 December 13. *Astroparticle Physics*, 31(6):407–411, 2009.

[13] J. H. Jenkins, E. Fischbach, J. B. Buncher, J. T. Gruenwald, D. E. Krause, and J. J. Mattes. Evidence of correlations between nuclear decay rates and Earth-Sun distance . *Astroparticle Physics*, 32(1):42–46, 2009.

[14] J. Klinger and V. A. Kudryavtsev. Muon-Induced Neutrons Do Not Explain the DAMA Data. *Physical Review Letters*, 114:151301, Apr 2015.

[15] W. R. Leo. *Techniques for Nuclear and Particle Physics Experiments: A How-to Approach*. Springer, 1994.

[16] National Institute of Standards and Technology. Radionuclide half-life measurements.
`https://www.nist.gov/pml/radionuclide-half-life-measurements-data`. (2017-02-08).

[17] J. Nistor, E. Fischbach, J. T. Gruenwald, D. Javorsek II, J. H. Jenkins, and R. H. Lee. Time-Varying Nuclear Decay Parameters and Dark Matter, 2013. arXiv:1307.7620v2 [hep-ph].

[18] E. B. Norman, E. Browne, H. A. Shugart, T. H. Joshi, and R. B. Firestone. Evidence against correlations between nuclear decay rates and Earth-Sun distance. *Astroparticle Physics*, 31(2):135–137, 2009.

[19] E. B. Podgoršak. *Radiation Physics for Medical Physicists*. Springer, 2010.

[20] E. Rutherford, J. Chadwick, and C. D. Ellis. *Radiations from Radioactive Substances*. Cambridge University Press, 1930.

[21] H. Siegert, H. Schrader, and U. Schötzig. Half-life measurements of Europium radionuclides and the long-term stability of detectors. *Applied Radiation and Isotopes*, 49(9-11):1397–1401, 1998.

[22] P. A. Sturrock, E. Fischbach, and J. Jenkins. Analysis of Beta-Decay Rates for ^{108}Ag, ^{133}Ba, ^{152}Eu, ^{154}Eu, ^{85}Kr, ^{226}Ra, and ^{90}Sr, Measured at the Physikalisch-Technische Bundesanstalt from 1990 to 1996. *The Astrophysical Journal*, 794(1):42, 2014.

[23] S.Y.F. Chu, L.P. Ekström, and R.B. Firestone. The Lund/LBNL Nuclear Data Search. `http://nucleardata.nuclear.lu.se/toi/`. (2017-02-08).

[24] The XENON Collaboration, E. Aprile et al. Exclusion of leptophilic dark matter models using XENON100 electronic recoil data. *Science*, 349(6250):851–854, 2015.

[25] The XENON Collaboration, E. Aprile et al. Search for Event Rate Modulation in XENON100 Electronic Recoil Data. *Physical Review Letters*, 115:091302, Aug 2015.